

# Morphology of Intermetallic Compounds in Al-Si-Fe Alloy and Its Control by Ultrasonic Vibration\*

Yoshiaki Osawa, Susumu Takamori, Takashi Kimura,  
Kazumi Minagawa and Hideki Kakisawa

National Institute for Materials Science, Tsukuba 305-0047, Japan

Iron impurity in aluminum alloys forms coarse needle-shaped intermetallic compounds during solidification and hampers the recycling process. To control the morphology of the material microstructure, an experiment was carried out where ultrasonic vibration was applied to the melt during solidification. Aluminum-Silicon-Iron alloys containing 4 mass% iron were melted and solidified. The primary crystals that formed from the melts were intermetallic compounds that were identified as  $\text{Al}_3\text{Fe}$ ,  $\alpha\text{-AlSiFe}$  ( $\text{Al}_{7.4}\text{SiFe}_2$ ) and  $\beta\text{-AlSiFe}$  ( $\text{Al}_9\text{Si}_2\text{Fe}_2$ ). The refinement of these intermetallic compounds was thought to occur with the application of ultrasonic vibration. Accurate results were obtained when the vibration was applied at the liquidus temperature. The liquidus temperatures of the Al-6~15Si-4Fe alloys were in the range of 945 to 955 K regardless of the silicon content and that of the Al-18Si-4Fe alloy was 977.2 K.

Coarse plate-like intermetallic compounds formed in Al-6 mass%Si-4 mass%Fe and Al-12 mass%Si-4 mass%Fe alloys, which can be refined by the application of ultrasonic vibration on crossing the liquidus temperature on cooling. The coarse columnar structure of an Al-18 mass%Si-4 mass%Fe alloy was modified to a fine grained structure. [doi:10.2320/matertrans.F-MRA2007874]

(Received November 22, 2006; Accepted June 7, 2007; Published July 25, 2007)

**Keywords:** aluminum-silicon-iron alloy, ultrasonic vibration, intermetallic compound, fine grain, deep etching,  $\alpha\text{-AlSiFe}$ ,  $\beta\text{-AlSiFe}$

## 1. Introduction

Recycling is important for the establishment of a “resource recycling-based society”. However, with increasing technological advances, the demands for the use of composite or combined materials in the production of goods make it difficult to achieve a high degree of recycling of these products. For example, the bodies of steel cans for beverages are made of steel but their lids are made of an aluminum alloy. The cylinder block of the aluminum alloy that surrounds the cast iron liner in automobile engines is another example and contains composite parts of cast iron and aluminum. The parts made of aluminum alloy and iron still remain even after shredding and separating. If this type of scrap is incorporated into the raw material, iron will be mixed with aluminum forming undesirable brittle intermetallic compounds.<sup>1-4)</sup> The solubility of iron into solid aluminum is low, only 0.005 mass% (hereafter abbreviated as %) even at 723 K.<sup>2)</sup> Although the amount of iron that is allowed as an impurity depends on the type of material, the amount of iron in general should not exceed 1% to prevent its penetration into the die even for a die casting process with high tolerance.<sup>4)</sup> If steel is introduced into aluminum in the form of composites, the iron content increases and the intermetallic compounds will form coarse plates.<sup>1)</sup> If the intermetallic compound could be dispersed finely and uniformly, mechanical properties such as ductility will not deteriorate much, and the increase in heat resistance which is similar to that in the Al-8%Fe-4%Ce alloy produced by powder metallurgy can be expected.<sup>3)</sup> Thus, an aluminum alloy containing high iron impurity can be used as a raw material if the iron intermetallic compound is finely dispersed by some solidification process.

The authors have carried out some experiments in which

the grain refinement of Al-Si alloys can be achieved by applying ultrasonic vibration. The grain refinement of the iron intermetallic compound in the Al-Si-Fe alloy is also expected to occur by using ultrasonic vibration. The grain refining mechanism from previous experiments on Al-Si alloys was the promotion of nucleation by the application of ultrasonic vibration.<sup>5-7)</sup> The primary crystals of Al-Si-Fe nucleated as intermetallic compounds when the iron content was high. The liquidus temperatures of these primary crystals were provided in the compilation of the ternary phase diagrams by G. Petzow and G. Efenberg.<sup>8)</sup> However, some discrepancies between the cross-sectional phase diagram corresponding to the 4% Fe of the Al-Si-Fe alloy and the liquidus temperature from the isothermal diagram were observed. Thus, measuring the nucleation temperature of the primary iron intermetallic compound was necessary to establish the optimal zone for the application of ultrasonic vibration.

With the aim of using scraps of aluminum alloys containing large amounts of iron, we measured the nucleation temperature of intermetallic compounds and investigated the compounds formed in Al-Si-Fe alloys. At the same time, the morphological changes of these intermetallic compounds were investigated through the application of ultrasonic vibration.

## 2. Experimental

### 2.1 Preparation of Al-Si-Fe master alloy

To obtain an Al-Si alloy with high iron content, specimens with 1%, 2%, and 4% iron were prepared and analyzed. The 4% Fe alloy was selected for the experiment because it fulfilled the condition of the formation of coarse needle-like Al-Si-Fe intermetallic compounds. Based on the cross-sectional phase diagram for the Al-Si alloy with 4% Fe,<sup>8)</sup> the amount of Si was varied from 3% to 18% to produce an Al-X%Si-4%Fe alloy (hereafter referred to as the master

\*This Paper was Originally Published in Japanese in J. JFS 78 (2006) 65-70.

Table 1 The chemical composition of these master alloys. (mass%)

Alloy	Si	Fe	Cu	Ni	Zn	Mn	Mg	Cr	Ti
Al-6%Si-4%Fe	5.99	4.16	0.005	0.004	0.002	0.015	0.003	0.004	0.017
Al-12%Si-4%Fe	11.9	4.11	0.003	0.004	0.003	0.014	0.002	0.004	0.010
Al-18%Si-4%Fe	17.6	4.05	0.004	0.004	0.001	0.017	0.011	0.004	0.010

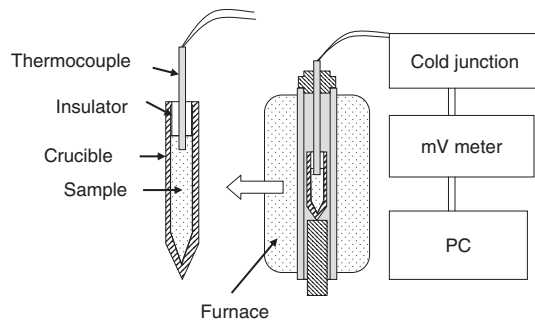


Fig. 1 Schematic of thermal analysis of Al-Si-Fe alloys.

alloy). An Al-25%Si master alloy, a 99.9%Al and an Al-50%Fe master alloy were melted in graphite crucibles using a high frequency induction furnace to produce 2 kg of the master alloy. The melt was kept at 1273 K for 300 s to ensure complete dissolution, and then cast at 1123 K into several molds with an internal diameter of 10 to 25 mm and a height of 250 mm. The result of the chemical composition of these master alloys is shown in Table 1.

## 2.2 Measurement of the liquidus line

Precise thermodynamic analytical experiments were carried out according to the Al-Si-4%Fe alloys cross-sectional phase diagram in the literature,<sup>8)</sup> and master alloys with Si content varying from 3% to 18%, at an increment of 3%, were produced. To prevent segregation, the master alloy was cast in metal dies with an internal diameter 10 mm, quenched, and cut into samples with a length of 50 mm for temperature measurements. Figure 1 shows an outline of the experiment. A hole with a diameter of 2 mm and a length of 10 mm was drilled to insert a thermocouple with a diameter 0.1 mm into one end of each specimen. The samples were introduced into an alumina Tammann crucible (12 mm id. and 85 mm long), which was put into an isothermal section of 30 mm id. and 150 mm long at the center of an electric furnace. After melting at 1123 K and holding for 300 s, the melt in the crucible was cooled at a cooling rate of about 0.19 K/s. The electromotive force of the thermocouple was measured and recorded with a digital multimeter. Thermal analysis was also carried out using a differential scanning calorimeter (DSC) for comparison. DSC experiments were performed on samples with a weight of 0.04 g and a heating rate of 0.1 K/s.

## 2.3 Cooling rate and morphology of intermetallic compounds

Changes in the morphology of intermetallic compounds in Al-Si-Fe alloys that were induced by changes in the cooling rate were investigated. The selected alloys were Al-X%Si-4%Fe, where X was 6%, 12%, and 18%. 240 g batches of the

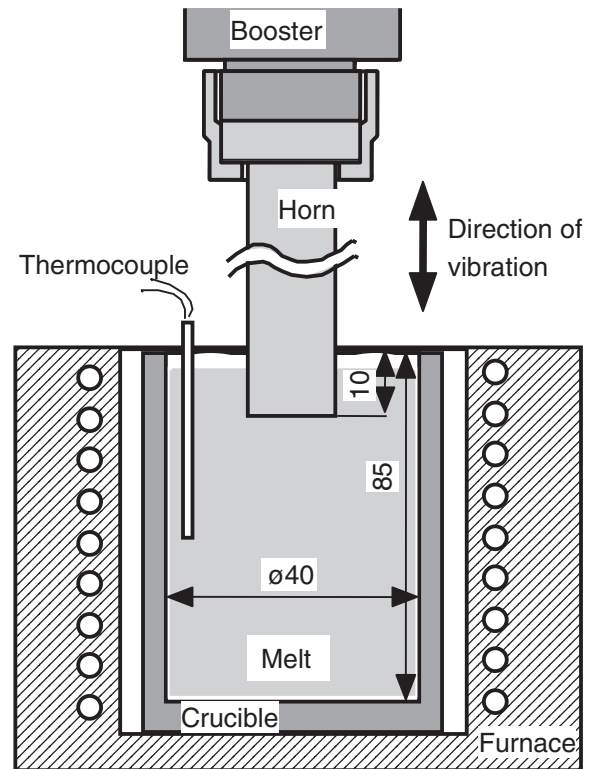


Fig. 2 Arrangement of a horn, a crucible and melting furnace for applying ultrasonic vibration to Al-Si-Fe alloys during the solidification state.

master alloy were placed into a high frequency furnace and melted at 1273 K. Then they were poured into metal molds with diameters of 10 and 20 mm and a height of 250 mm, and into an alumina crucible with a diameter of 40 mm for casting at 1173 K. The cooling rate in the solidification process was measured with an R thermocouple with a diameter of 0.1 mm. Alumina cement was used to fix the thermocouple from the center of the molds. The cooling rate was in the range of 0.02 to 170 K/s. Samples for optical microscopy were collected from the center of the cast.

## 2.4 Application of ultrasonic vibration

Ultrasonic vibration was applied to the melt through a horn using equipment with an output of 1.2 kW and a frequency of 19 kHz. A Sialon horn with a diameter of 20 mm and a length of 288 mm was used. The amplitude of the horn tip was approximately 20  $\mu$ m. Figure 2 shows the relative positions of both the horn and the metal mold in the ultrasonic vibration equipment. A high frequency furnace was used to melt 240 g of the master alloy in alumina crucibles with an internal diameter of 40 mm and a length of 85 mm at 1123 K, and the horn was immersed to a depth of 10 mm from the melt surface. The cooling started after the temperature was kept at 1123 K for 300 s. When the temperature reached 973 K, the

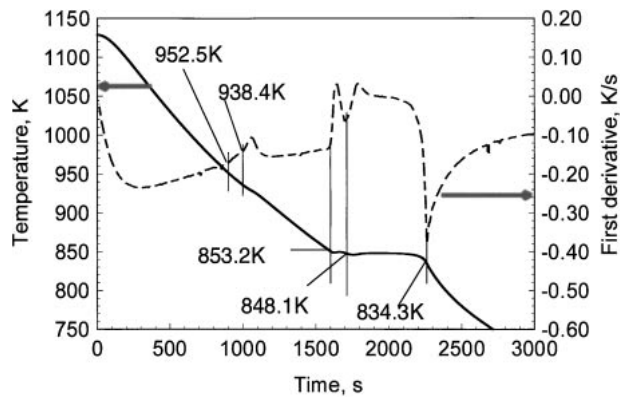


Fig. 3 Plot of thermal analysis data obtained for an Al-12Si-4Fe alloy.

high frequency generator of the ultrasonic vibration equipment was started, and vibration was applied until 873 K. At 873 K the horn was pulled from the melt. To determine the effect of the temperature in the application of ultrasonic vibration, the vibration was applied in the temperature range both above and below the liquidus temperature of the master alloy, Al-X%Si-4%Fe. To determine the optimum range of temperature for the application of ultrasonic vibration, vibration was applied 1) in the temperature range from 973 to 923 K, where the primary crystals of AlSiFe intermetallic compounds start to form, and 2) in the range from 923 to 873 K. To observe the longitudinal cross section, the ingots were vertically cut in half after solidification. At the same time, samples were collected from the center of the ingot for microstructure observation. The distribution and the identification of the intermetallic compounds were carried out by EPMA.

## 2.5 Observation of intermetallic compound microstructure after immersion corrosion treatment

To study the three-dimensional morphology of the intermetallic compounds formed at different cooling rates during the application of ultrasonic vibration, the aluminum matrix was removed leaving only the intermetallic compounds. A corrosion treatment was carried out at the end, in which the samples were immersed in a 40%NaOH aqueous solution at room temperature for 3.6 ks. Scanning electron microscopy was used to assess the morphology of the remaining intermetallic compounds, the eutectic, and the silicon phase.

## 3. Results

### 3.1 Measurement of the liquidus temperature

Figure 3 shows an example of the results from the thermal analysis on the Al-12%Si-4%Fe alloy cooled from 1123 K at a cooling rate of approximately 0.19 K/s. The inflection points on the cooling curve are shown by the dashed line in the differentiated curve. Although there is no inflection point on the cooling curve at 994 K, which is the liquidus temperature according to the ternary phase diagrams compiled by G. Petzow and G. Effenberg,<sup>8)</sup> there is a small inflection point at 952.5 K, which is assumed to be the liquidus temperature. At 938.4 K there is a small inflection point, and the Al-Si eutectic solidification is assumed to start

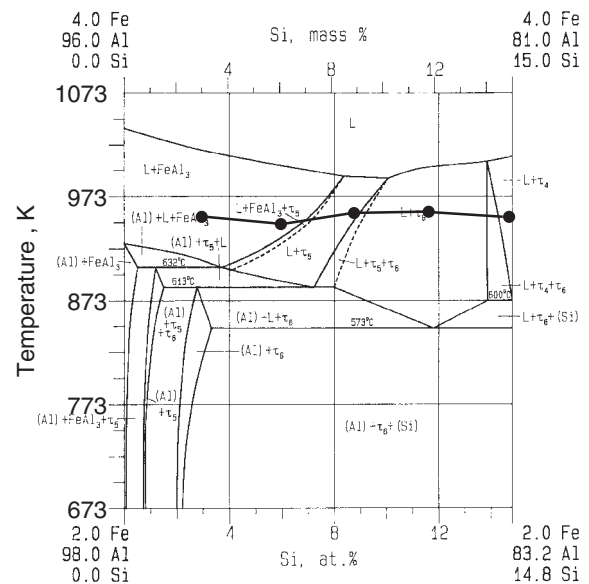


Fig. 4 Ternary alloys phase diagram of the Al-Si-Fe system at 4.0 mass%Fe.

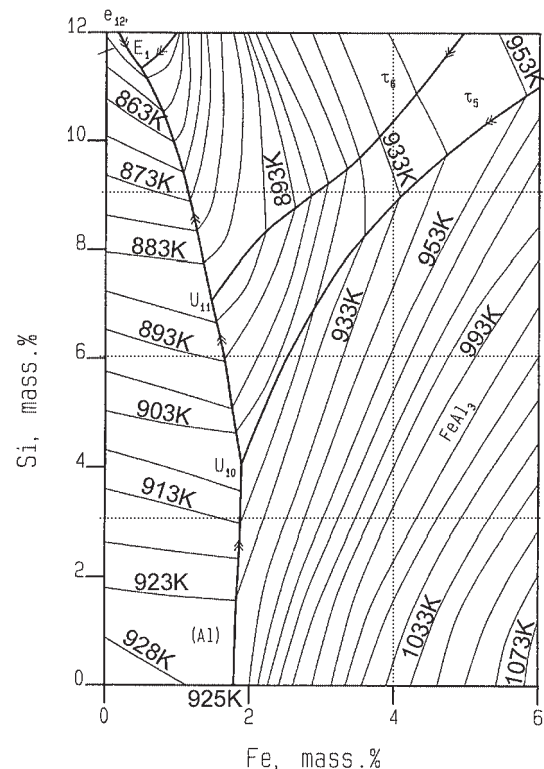


Fig. 5 Liquidus surface of the Al-corner of an Al-Si-Fe system.

at 853.2 K. According to the phase diagram in the literature,<sup>8)</sup> an intermetallic compound,  $\tau_6$  ( $\beta$ -AlSiFe ( $\text{Al}_9\text{Si}_2\text{Fe}_2$ )), was crystallized within the liquid phase from 994 K until the Al-Si eutectic temperature. The latent heat emission corresponding to the crystallization of  $\beta$ -AlSiFe was low under the calorimetry conditions in this work. Figure 4 shows a ternary phase diagram of the Al-Si-Fe alloy<sup>8)</sup> corresponding to 4%Fe, and Fig. 5 shows a plot of the liquidus temperature from the same literature.<sup>8)</sup> The measured liquidus temperature points were plotted on the lines shown in Fig. 4, and they were

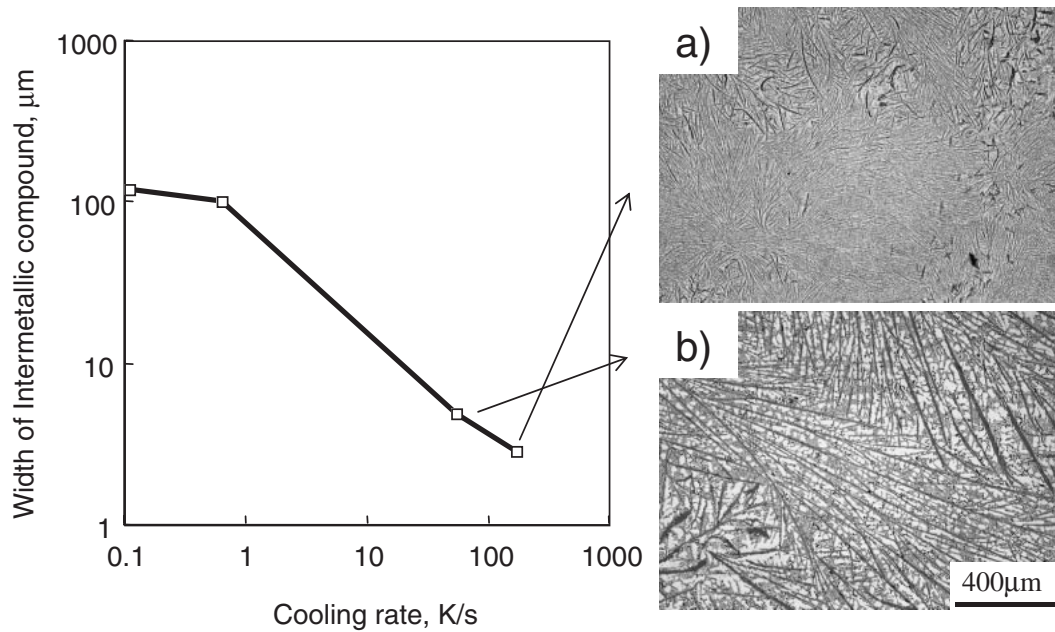


Fig. 6 Relationship between the width of an intermetallic compound of an Al-12Si-4Fe alloy and the cooling rate.

found to exhibit almost constant values such as 952.5 K, 948.6 K, 952.4 K, 952.2 K, and 952.6 K even though the Si content changed from 3%, 6%, 9%, 12% to 15%. For a Si content of 18%, the liquidus temperature in the literature<sup>8)</sup> shown in Fig. 5 was a little higher at 977.2 K. This liquidus temperature measurement DSC was of same values. Here  $\tau_4$  and  $\tau_5$  denote  $\text{Al}_3\text{Si}_3\text{Fe}$  and  $\text{Al}_{7.4}\text{SiFe}_2$ ,<sup>8)</sup> respectively. The liquidus temperature values obtained in this experiment is considered to be the liquidus temperature for the following experiments that involve the application of vibration.

### 3.2 Changes in morphology of intermetallic compounds with cooling rates

Figure 6 shows the changes in the thickness of the intermetallic compound with the cooling rate for an Al-12%Si-4%Fe alloy. The vertical axis shows the average thickness of the needle-like intermetallic compounds observed by optical microscopy. An increase in the cooling rate only has the effect of narrowing the width and does not change the needle-like shape. The results show that a) for specimens solidified in a metal mold having an inner diameter of 10 mm at the fastest cooling rate of 170 K/s, the average thickness of the needle-like intermetallic compounds was 2.9  $\mu\text{m}$ ; b) for specimens solidified in a metal mold having an inner diameter of 20 mm at a cooling rate of 56 K/s, an extremely thin feathery structured needle of intermetallic compounds was observed with a thickness of only 4.9  $\mu\text{m}$ . When the cooling rate was low, as in the solidification in 40 mm diameter alumina crucibles cooled in air, the intermetallic compounds precipitated as large needle-like particles with a length of 5,000–10,000  $\mu\text{m}$ . The thickness was approximately 100  $\mu\text{m}$ , and the aspect ratio was lower than 0.01.

When the melt in the crucible was cooled in the furnace and solidified at a cooling rate down to 0.11 K/s, the intermetallic compounds formed coarse particles that were almost the same size as those that resulted from a cooling rate

of 0.64 K/s. For Si content of 6 to 18%, the primary crystals of the intermetallic compound were extremely thin and formed a feathery structure at cooling rates of 50–170 K/s. In the Al-18%Si sample at a fast cooling rate, the intermetallic compounds formed a feathery structure (very fine needle-like structure), and Si precipitated as fine particles to be dispersed among the feathery structure with an increase in the cooling rate.

### 3.3 Structural control of intermetallic compounds through application of ultrasonic vibration

Figure 7 shows the optical micrographs of the center of the ingot sample after solidification of several Al-X%Si-4%Fe alloys. From the left side, the images correspond to 6%Si, 12%Si, and 18%Si alloys, respectively. The upper section corresponds to solidification without ultrasonic vibration, and the bottom section corresponds to solidification with ultrasonic vibration applied in the temperature range of 973 to 873 K. When ultrasonic vibration was not applied, the samples containing 6%Si and 12%Si displayed coarse needle-like structures. In particular, the intermetallic compounds of 12%Si alloy crystallized into coarse particles with a length of 10 mm, whereas the intermetallic compound and the hypereutectic structure in the 18%Si alloy formed coarse particles. After the application of ultrasonic vibrations in the 6%Si alloy, image analyses of the intermetallic compound showed an average equivalent diameter of 77  $\mu\text{m}$ . The average equivalent diameter in the 12%Si alloy was 59  $\mu\text{m}$ , and in the 18%Si alloy, the intermetallic compound appeared as thin rectangular particles with an average equivalent diameter of 65  $\mu\text{m}$ . Thus, the composition of the intermetallic compound was independent of ultrasonic vibration. The intermetallic compound of 6%Si a) and d) was coarse needle-like and round  $\alpha\text{-AlSiFe}$  ( $\tau_5$ :  $\text{Al}_{7.4}\text{SiFe}_2$ ), respectively, with a formation of a very thin layer of  $\beta\text{-AlSiFe}$  ( $\tau_6$ :  $\text{Al}_9\text{Si}_2\text{Fe}_2$ ) on the surface. In 12%Si b) and e), the intermetallic compound was coarse needle-like and large  $\beta\text{-AlSiFe}$ , respectively. In



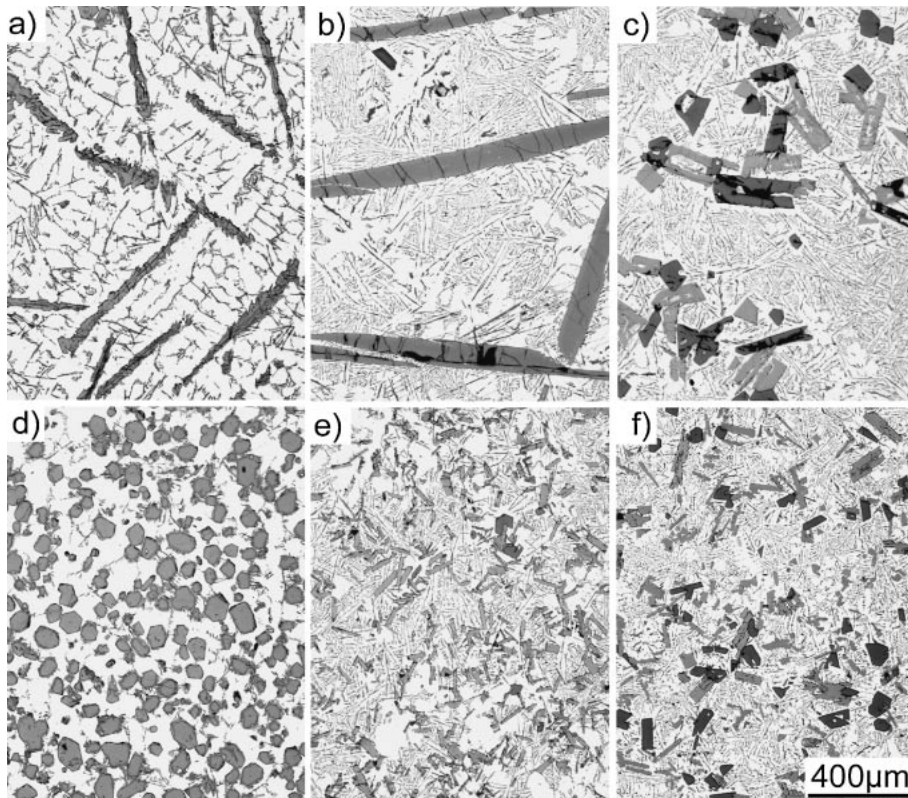


Fig. 7 Effect of ultrasonic vibration during solidification on a primary intermetallic compound of Al-Si-Fe alloys. (a), (d) Al-6Si-4Fe, (b), (e) Al-12Si-4Fe, c,f:Al-18Si-4Fe. (a), (b), (c). Without vibration. (d), (e), (f) With vibration at 973 K~873 K.

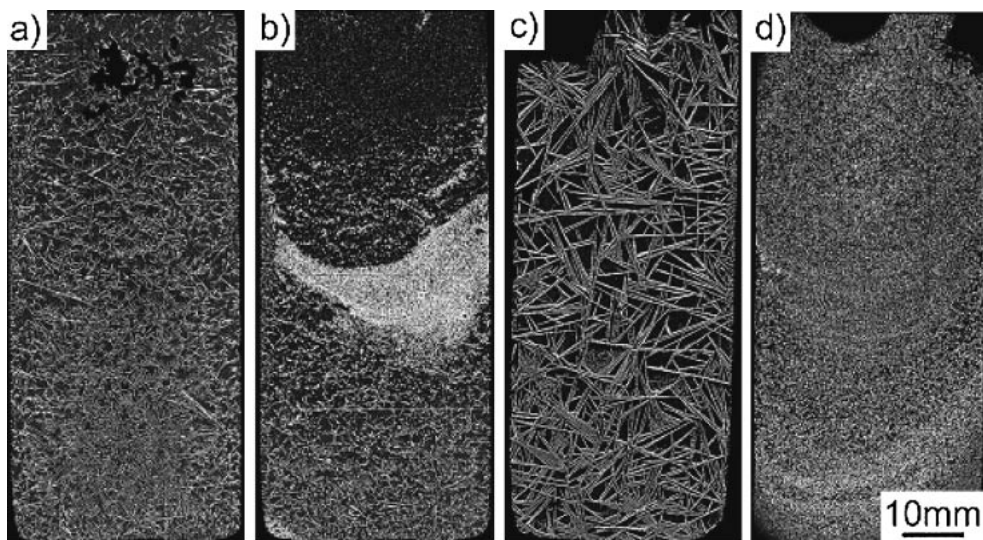


Fig. 8 EPMA mapping for iron on the longitudinal cross section of Al-Si-Fe alloys. (a), (b) Al-6Si-4Fe, (c), (d) Al-12Si-4Fe. (a), (c). Without vibration. (b), (d) With vibration at 973 K~873 K.

18%Si c), the light gray phase is  $\beta$ -AlSiFe, with regions of  $\delta$ -AlSiFe ( $\text{Al}_3\text{Si}_2\text{Fe}$ ). The dark gray phase shows large grains of Si.

Figure 8 corresponds to an EPMA Fe- $K\alpha$  mapping of the whole ingot solidified with the application of ultrasonic vibration for Al-6%Si-4%Fe and Al-12%Si-4%Fe alloys. EPMA analysis shows that Fe was present in almost all the intermetallic compounds, and that the distribution of the

chemical was established in compounds along the transversal section of the ingot. When ultrasonic vibration was not applied, a coarse grain structure formed, whereas the application of ultrasonic vibration resulted in a fine microstructure that was evenly distributed inside the ingot. In the Al-6%Si-4%Fe alloy, layers of intermetallic compounds accumulated from the bottom of the crucible. This layer structure was attributed to the effect of the radiation pressure

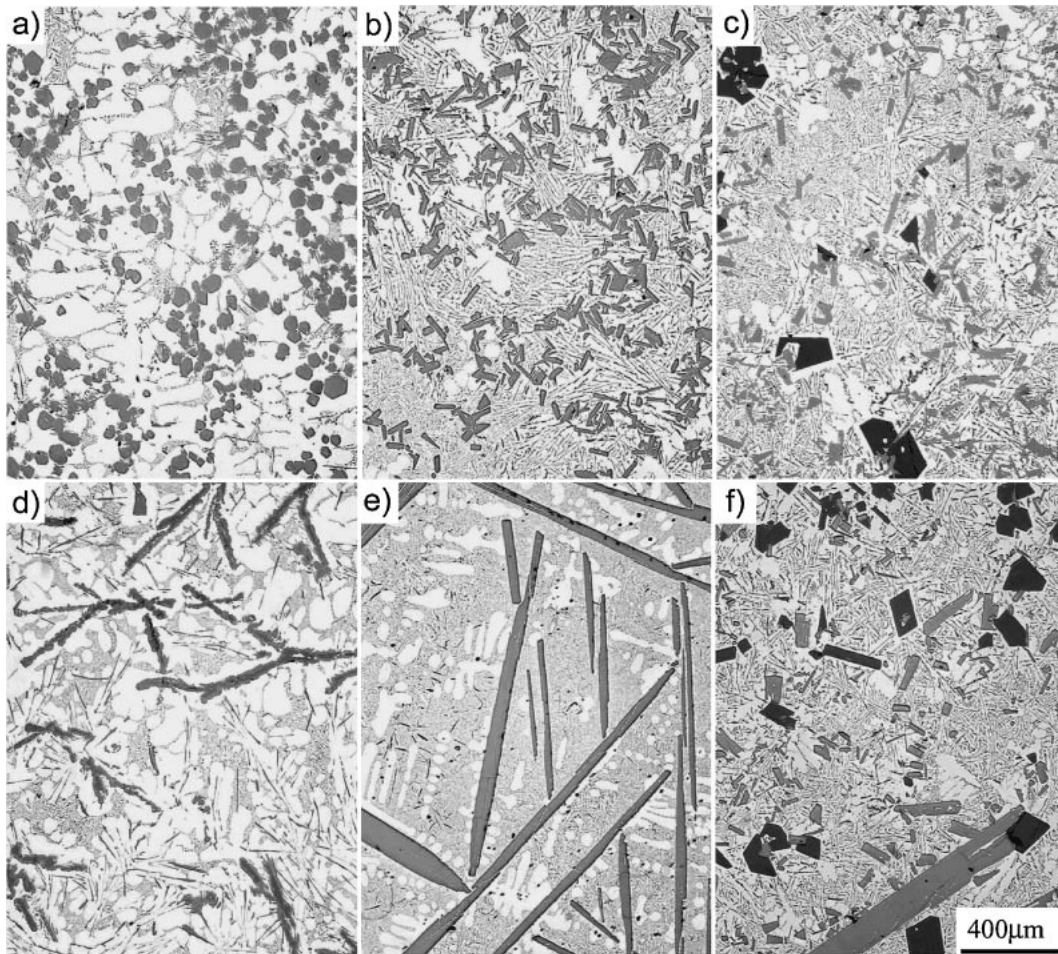


Fig. 9 Effect of ultrasonic vibration during solidification on a primary intermetallic compound structure of an Al-Si-Fe alloy. (a), (d) Al-6Si-4Fe, (b), (e) Al-12Si-4Fe, (c), (f) Al-18Si-4Fe. (a), (b), (c) 973 K~923 K ultrasonic vibration is applied. (d), (e), (f) With vibration at 923 K~873 K.

and acoustic flow generating from the tip of the horn, which caused structure refining, the same as the distribution of fine particles of Si in the hypereutectic Al-18%Si.<sup>5-7)</sup> The flow of the melt caused segregation and induced the formation of this layer of precipitates at the bottom of the ingot.

Figure 9 shows some microscopic photographs, in which the temperature where the ultrasonic vibration was applied was varied to evaluate the effects of temperature on the morphology of the primary crystals of intermetallic compounds. The upper section corresponds to ultrasonic vibration applied at 973–923 K, followed by the removal of the horn and solidification. The observed fine structure of primary crystals of intermetallic compounds is similar to those of the specimens in Fig. 7 with ultrasonic vibration applied at 973–873 K. The structure of the Al-6%Si-4%Fe alloy consists of fine particles and that of Al-12%Si-4%Fe and Al-18%Si-4%Fe alloys are of fine platelets. In the bottom section, when ultrasonic vibration is applied in the 923–873 K range below the liquidus temperature, the photos show that intermetallic compounds do not have the fine structure of the primary crystals of AlSiFe. Although the primary crystals of the intermetallic compounds were finer than those in the specimens without any ultrasonic vibration application in Fig. 7, they still formed a coarse needle-like structure.

### 3.4 Microstructures of intermetallic compounds after immersion corrosion tests

Figure 10 shows SEM photographs of the samples which have undergone immersion corrosion after ultrasonic vibration was applied. The intermetallic compound that appeared as coarse needles in the optical micrographs of Al-6%Si-4%Fe and Al-12%Si-4%Fe alloys that did not receive any ultrasonic vibration now appear as coarse platelets. After the application of vibration, the shape of the intermetallic compound in the Al-6%Si-4%Fe alloy became almost spherical, while they appeared as fine short platelets in the Al-12%Si-4%Fe alloy and minute short platelets in the Al-18%Si-4%Fe alloy. The Al-Si-4%Fe alloy was poured into a metal die with a diameter of 10 mm to be quenched before undergoing immersion corrosion treatment, and the SEM images of the intermetallic compound showed that the fine feathery structure observed with the optical microscope was made up of extremely thin platelets.

## 4. Discussion

### 4.1 Liquidus temperatures for Al-Si-Fe alloys

Because of the low solubility of iron in aluminum, almost all the iron added to an Al-Si alloy form intermetallic compounds. As shown in Fig. 3, the liquidus temperature for

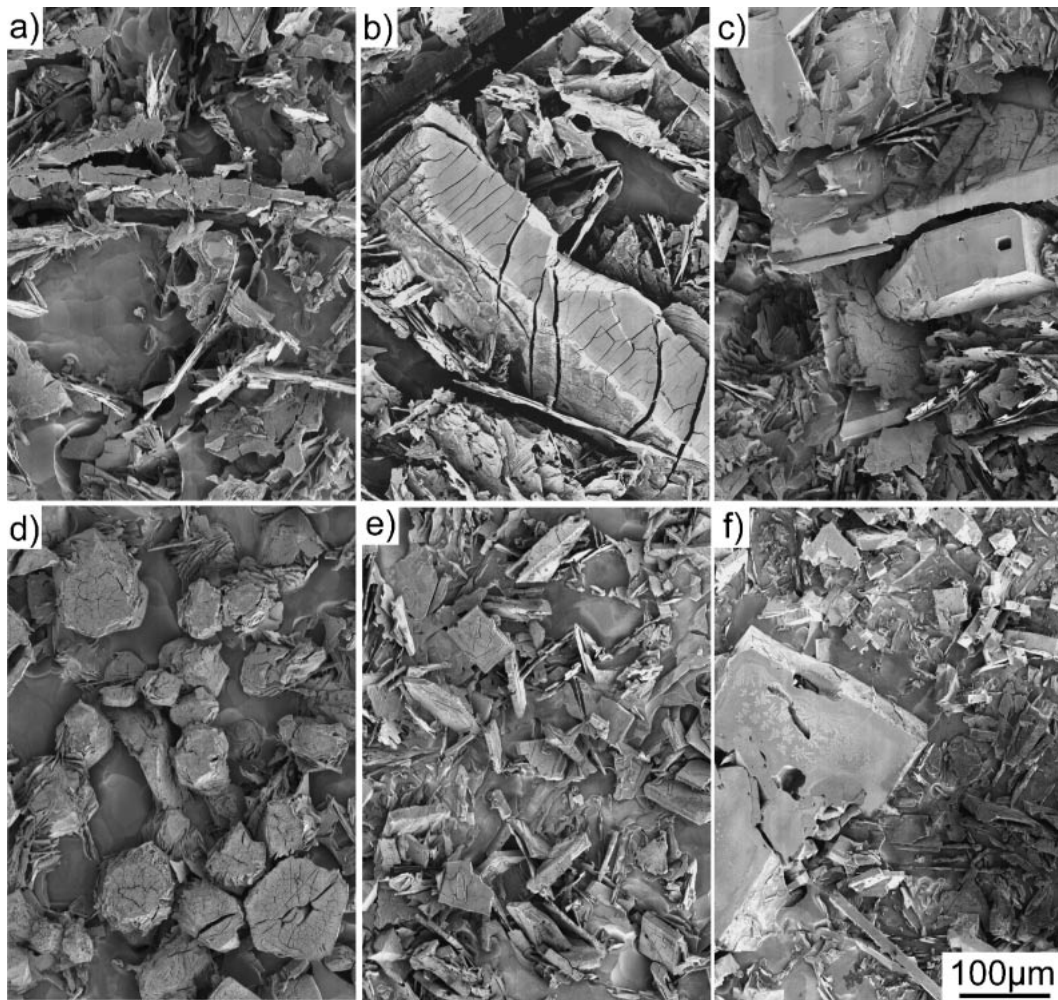


Fig. 10 SEM observation of the specimen etched in 40 mass%NaOH solution for 3.6 ks. (a), (d) Al-6Si-4Fe, (b), (e) Al-12Si-4Fe, (c), (f) Al-18Si-4Fe. (a), (b), (c). Without vibration. (d), (e), (f) With vibration at 973 K~873 K.

an Al-Si-4%Fe alloy is difficult to identify, since the latent heat emission corresponding to crystallization is low. The liquidus temperature reported in the ternary phase diagrams for an Al-Si-4%Fe alloy<sup>8)</sup> appears at higher temperatures than those observed in this study. The liquidus temperature in the diagram (Fig. 4) for the 6%Si alloy is located at 999.6 K, while our experimental value was at 948.6 K, 51 K lower than those in the diagrams. For the 12%Si alloy, the value in the literature<sup>8)</sup> is 998.5 K, 46 K higher than our experimental value of 952.5 K.

The liquidus temperature of the Al-Si-4%Fe alloy that was used in the present experiments was approximately 950 K regardless of the Si content and was close to the value in the corresponding ternary phase diagram<sup>8)</sup> (Fig. 5). Thermal analyses using DSC and detailed temperature measuring experiments provided the same values. The present research was carried out based on this low liquidus temperature. In the Al-6-18%Si-4%Fe alloy, the primary crystals that formed at the liquidus temperature were intermetallic compounds, which have been identified as  $\text{Al}_3\text{Fe}$ ,  $\alpha\text{-AlSiFe}$  ( $\text{Al}_{7.4}\text{SiFe}_2$ ) and  $\beta\text{-AlSiFe}$  ( $\tau_6$ :  $\text{Al}_9\text{Si}_2\text{Fe}_2$ ).<sup>8)</sup> For example, the intermetallic compound that formed at the liquidus temperature on the cooling line during solidification is said to be  $\beta\text{-AlSiFe}$  for Al-12%Si-4%Fe in Fig. 4.

In these experiments where the cooling rate was 0.19 K/s, the emission of latent heat of this intermetallic compound was relatively small for solidification and difficult to identify. Even with the changes in the Si contents and with the formation of diverse intermetallic compounds, the inflection of the cooling curve caused by the emission of latent heat for solidification was very small. However, when ultrasonic vibration was applied under a cooling rate of 0.64 K/s, the cooling curve showed a noticeable bending that was assumed to be the liquidus temperature as in the Al-12%Si-4%Fe alloy shown in Fig. 11. The liquidus temperature without any vibration was 932.3 K, i.e., 20 K lower than the values in Fig. 3, which corresponds to supercooling during solidification. The application of ultrasonic vibration induced an inflexion point at 954.7 K, which is close to the value shown in Fig. 3, and resulted in a massive precipitation of primary crystals. At this point, the temperature difference was 22.4 K. When ultrasonic vibration was applied, the melt was dynamically stimulated to promote nucleation, and the supercooling phenomenon was able to be hindered.<sup>9)</sup> From these observations, the liquidus temperature for the Al-12%Si-4%Fe alloy was thought to be in the vicinity of 954.7 K. If supercooling does not occur by the application of ultrasonic vibration, the liquidus temperature would be 45 K

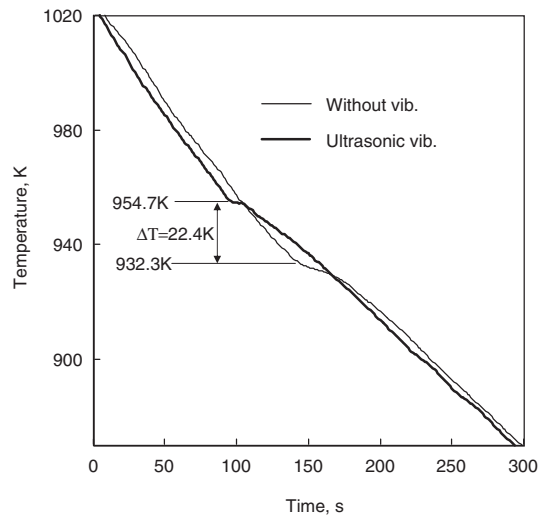


Fig. 11 Cooling curve of an Al-12Si-4Fe alloy solidified in the mold.

lower than the values on the cross-sectional phase diagram (Fig. 4) for 4%Fe in the ternary phase diagram in the literature;<sup>8)</sup> however, it would agree with the 952.5 K value that was obtained in this work as shown in Fig. 3.

The ternary phase diagram is also shown by Phillips and Varley,<sup>10)</sup> and Watanabe and Sato.<sup>11)</sup> The value from Phillips and Varley is similar to that in Fig. 5, while the value from Watanabe and Sato is similar to that in Fig. 4. However, we are not certain which phase diagram is correct. In this research, a commercial alloy is used, and the effect of impurities is assumed to be small when considering the phase diagrams. Detailed thermal analysis also cannot determine the phase change with certainty. In this research, we were able to determine the liquidus temperature when ultrasonic vibration was applied.

#### 4.2 Crystallization of intermetallic compounds in Al-Si-Fe alloys

Almost all the iron in the Al-Si alloy do not dissolve but crystallize as intermetallic compounds, which is clear from the EPMA results. In this section, crystallization of intermetallic compounds in the Al-12%Si-4%Fe alloy will be discussed. In this alloy, the primary crystals of the intermetallic compounds appear when crossing the liquidus line, and there is usually a large supercooling as shown in Fig. 11. Although the formation of nuclei of the intermetallic compounds at this liquidus temperature is difficult, large supercooling can initiate nucleation at once, which works as a driving force to promote the formation of coarse platelets. Very thin platelets with the feathery structure shown in Fig. 6 can be produced by quenching at a cooling rate of 50–170 K/s. Figure 9(b) shows that intermetallic compounds in specimens kept a fine particle structure after the application of ultrasonic vibration at the first stage of solidification in the temperature range of 973–923 K and cooling at 1 K/s. The application of ultrasonic vibration is known to stimulate nucleation<sup>5,6,9)</sup> and the fine particle structure of intermetallic compounds is thought to result from a large amount of nucleation. Figure 12 confirms this assumption and shows a quenched specimen after the application of ultrasonic

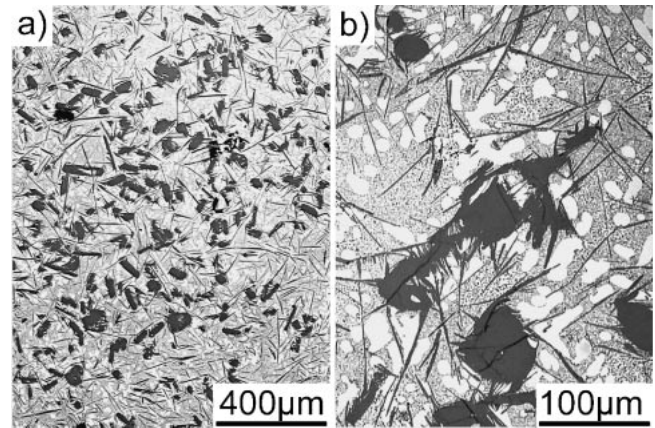


Fig. 12 Effect of ultrasonic vibration during solidification on a primary intermetallic compound in an Al-12Si-4Fe alloy. Ultrasonic vibration was applied at 973 K~953 K.

vibration at 973–953 K. Figure 12(b) is an enlargement of 12(a). The round particles are attributed to a massive precipitation of the intermetallic compound at 954.7 K as the effect from the application of ultrasonic vibration. The structure of the needle-like branches extending from the round particles correspond to the crystallized intermetallic compounds that developed when the primary crystals of the intermetallic compound were quenched from 953 K, and formed into needles from the new crystals of intermetallic compounds after maintaining their original shape. The portion corresponding to the needle-like branches growing out of the round particles was analyzed by image analysis. The area ratio of the needle-like branches was 5%. When the round particles of the intermetallic compound of specimens that have received ultrasonic vibration in Figs. 12 and 7(e) are compared, we find that crystallization in the vicinity of the liquidus temperature has reached 80%.

To control the microstructure in Al-Si-Fe alloys and to obtain fine particles of intermetallic compounds instead of platelets, ultrasonic vibration should be applied in the region located at both sides of the liquidus temperature. On the other hand, the large supercooling during quenching of these intermetallic compounds causes a structure of fine platelets to grow after the start of a massive nucleation. Therefore, to achieve the fine structures of the intermetallic compounds, it is important to promote the formation of a large amount of crystal nuclei during the application of ultrasonic vibration and to cool them gradually to ensure the growth of round grains.

#### 5. Conclusions

Morphology and morphological control of AlSiFe intermetallic compounds that crystallize in Al-Si-Fe alloys were investigated.

- (1) The intermetallic compounds form coarse platelets (appearing as needles on the observed surface) in the Al-6%Si-4%Fe and Al-12%Si-4%Fe alloys, while they form a massive coarse structure in the Al-18%Si-4%Fe alloy.
- (2) The liquidus line for the nucleation of primary crystals



of the intermetallic compounds is 952.5 K in Al-Si-Fe alloys.

- (3) Supercooling occurs easily during the crystallization of intermetallic compounds in Al-Si-Fe alloys. In the Al-12%Si-4%Fe alloy, with a cooling rate of 0.64 K/s, the liquidus temperature was modified approximately 20 K to 932.3 K by supercooling. The application of ultrasonic vibration resulted in a liquidus line that coincided with the experimental results with a value of 954.7 K.
- (4) Regardless of the cooling rate, all the intermetallic compounds formed platelets in the Al-6%Si-4%Fe and Al-12%Si-4%Fe alloys. The compounds formed very thin platelets with high cooling rates.
- (5) The refinement of the intermetallic compounds that crystallize as the primary phase from the Al-Si-Fe alloy melts was made by applying ultrasonic vibration at their nucleation temperature.

### Acknowledgement

This research was financially supported by a Grant in Aid

for Scientific Research of the Ministry of Education, Culture, Sports, Science and Technology of Japan.

### REFERENCES

- 1) A. Kamio: Report of JFS Meeting **143** (2003) 49.
- 2) J. Jpn. Inst. Light Met. Ed.: "*Characterization and Structure of Aluminum*" (J. Jpn. Inst. Light Met.) (1991) 340.
- 3) M. Nishio, S. Nasu and Y. Murakami: J. Jpn. Inst. Met. **34** (1970) 1173.
- 4) T. Takahashi ed.: *Hitetsu Kinzokuzairyou Sentaku no Point* 2nd ed. (Japanese Standards Association, 2002) 69.
- 5) Y. Osawa, G. Arakane, S. Takamori, A. Sato and O. Ohashi: J. JFS **71** (1999) 98.
- 6) Y. Osawa, S. Takamori, G. Arakane, O. Umezawa, A. Sato and O. Ohashi: J. JFS **72** (2000) 187.
- 7) Y. Osawa and A. Sato: J. JFS **72** (2000) 733.
- 8) G. Petzow and G. Effenberg ed.: "*Ternary Alloys, Vol. 5*" (VCH) (1992) 434.
- 9) T. Okamoto and A. Suzuki trans.: "*Kinzoku no gyouko*" (Maruzen) (1971) 80.
- 10) H. W. L. Phillips and P. C. Varley: J. Inst. Metals **69** (1943) 317.
- 11) H. Watanabe and E. Sato: "*Jitsuyougoukinjoutaizusetsu*" (Nikkankougyousinbunsha) (1966) P215.